ESCAP/WMO
Typhoon Committee

Available online at www.sciencedirect.com

ScienceDirect

Tropical Cyclone Research and Review 12 (2023) 151–164

www.keaipublishing.com/tcrr

Recent progress in research and forecasting of tropical cyclone outer size

Benjamin A. Schenkel [a,b,c,*], Chris Noble [d], Daniel Chavas [e], Kelvin T.F. Chan [f,g,h], Stephen J. Barlow [i], Amit Singh [j], Kate Musgrave [k]

[a] *Cooperative Institute for Severe and High-Impact Weather Research and Operations, University of Oklahoma, Norman, OK, USA*
[b] *NOAA/OAR National Severe Storms Laboratory, Norman, OK, USA*
[c] *School of Meteorology, University of Oklahoma, Oklahoma, USA*
[d] *MetService, Wellington, New Zealand*
[e] *Department of Earth, Atmospheric, and Planetary Science, Purdue University, West Lafayette, IN, USA*
[f] *School of Atmospheric Sciences, Sun Yat-sen University, Southern Marine Science and Engineering Guangdong Laboratory (Zhuhai), Zhuhai, China*
[g] *Guangdong Province Key Laboratory for Climate Change and Natural Disaster Studies, Sun Yat-sen University, Zhuhai, China*
[h] *Key Laboratory of Tropical Atmosphere-Ocean System (Sun Yat-sen University), Ministry of Education, Zhuhai, China*
[i] *Joint Typhoon Warning Center, Pearl Harbor, Hawaii, USA*
[j] *Fiji Meteorological Service, Nadi, Fiji*
[k] *Cooperative Institute for Research in the Atmosphere, Fort Collins, CO, USA*

Available online 16 September 2023

Abstract

This review article summarizes the current understanding and recent updates to tropical cyclone outer size and structure forecasting and research primarily since 2018 as part of the World Meteorological Organization's 10th International Workshop on Tropical Cyclones. A more complete understanding of tropical cyclone outer wind and precipitation is key to anticipating storm intensification and the scale and magnitude of landfalling hazards. We first discuss the relevance of tropical cyclone outer size and structure, improvements in our understanding of its life cycle and inter-basin variability, and the processes that impact outer size changes. We next focus on current forecasting practices and differences among warning centers, recent advances in operational forecasting, and new observations of the storm outer wind field. We also summarize recent research on projected tropical cyclone outer size and structure changes by the late 21st century. Finally, we discuss recommendations for the future of tropical cyclone outer size forecasting and research.

Keywords: Tropical cyclones; Climate change; Operational forecasting; Outer size; Outer structure

1. Introduction

The life cycle of tropical cyclone (TC) outer wind size and structure has received increased focus given its importance to storm hazards including storm surge (Irish et al., 2008; Lin et al., 2014) and tornadoes (McCaul 1991; Paredes et al., 2021). Prior work has defined the TC outer region at radii far outside the storm center where winds are typically weak and

* Corresponding author. National Weather Center, 120 David L. Boren Blvd., Norman, OK 73072, USA.
E-mail address: benschenkel@gmail.com (B.A. Schenkel).
Peer review under responsibility of Shanghai Typhoon Institute of China Meteorological Administration.

Production and Hosting by Elsevier on behalf of KeAi

https://doi.org/10.1016/j.tcrr.2023.09.002

convection is sparse (Emanuel et al., 2004; Chavas et al., 2015). Compared to the rapid changes in TC intensity, the outer winds typically slowly increase throughout most of the storm life cycle (Merrill 1984; Weatherford and Gray 1988). Outer size is most frequently measured in operations using either the radii of 34-kt (R34), 50-kt (R50), or 64-kt winds (R64), or the radius of the outermost closed isobar (ROCI; Demuth et al., 2006; Knaff et al., 2014). In contrast, research has used many different metrics due to the limited availability of outer wind field observations throughout the storm life cycle (Liu and Chan 1999; Chavas and Emanuel 2010; Chan and Chan 2018). This review article builds upon the review of Chan and Chan (2018) by summarizing new advances in our understanding of TC outer size and structure, and its life cycle in both research and operations.

2. TC outer size and structure research

a) New insights into TC outer size and structure characteristics

TC outer size and structure are characterized by significant inter-basin and life cycle variability (Chan and Chan 2015; Chavas et al., 2016). On average, the largest and smallest sizes are observed over the western and eastern North Pacific, respectively (Fig. 1). Eastern North Pacific TCs also tend to be the most asymmetric, although most TCs have some degree of outer wind asymmetries (Zhang and Chan 2023). These differences in outer size among basins begin at genesis and continue throughout the storm life cycle with differing expansion rates and growth period lengths (Schenkel et al., 2018).

More broadly, TC outer size is generally smallest at genesis with expansion throughout most of the first half of the storm lifetime or longer (Schenkel et al., 2018). Lifetime maximum outer size generally occurs near or after the midpoint of TC lifetime following lifetime maximum intensity and the associated broadening of the radius of maximum winds (Schenkel et al., 2018; Wang and Toumi 2018a). Typically, those TCs with the largest outer size grow rapidly, while being among the longest-lived and traversing the greatest distances (Schenkel et al., 2018; Li et al., 2022). Nontrivial decreases in outer winds during the latter part of the TC lifetime are associated with cyclolysis or landfall, or typically either no change or additional decreases due to extratropical transition depending on the basin (Schenkel et al., 2018; Chen and Chavas 2020).

b) Recent advances in research quality TC outer size datasets

Recent work has focused on using a variety of datasets to investigate TC outer size and structure for a large sample of TCs (Schenkel et al., 2017; 2018; Mok et al., 2018). In particular, atmospheric reanalyses reasonably represent TC outer size albeit with a small bias and reduced variability compared to scatterometer data, although these issues are reduced in newer reanalyses (Schenkel et al., 2017; 2018; Mok et al., 2018; Bian et al., 2021; Zhang and Chan 2023). Recent work has also leveraged the radius of TC-induced sea-surface temperature (SST) cold wakes to provide global, multidecadal estimates of TC outer size as shown in Fig. 2 (Zhang et al., 2019; Wang and Toumi, 2021).

Additional research has applied a deep-learning approach to infrared satellite imagery to estimate R34 with improved performance compared to current operational products (Zhuo and Tan 2021). Fine-scale R34 estimates are now afforded by the satellite-based synthetic aperture radar, which has root-mean-

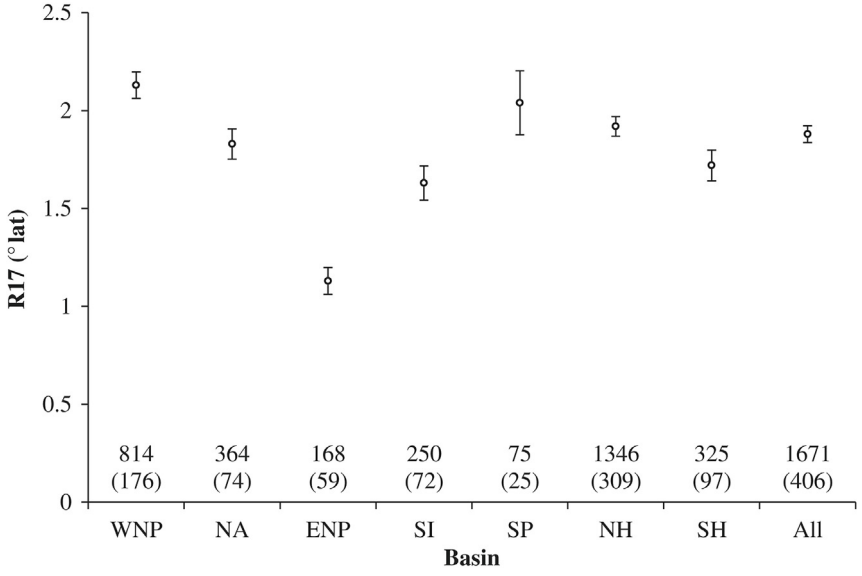

Fig. 1. Mean TC size by basin. Vertical bars represent the 95% confidence intervals in the t distribution. Numbers above the x-axis indicate the number of 6-h track points and the number of TCs in parentheses. Basins listed are the western North Pacific (WNP), North Atlantic (NA), eastern North Pacific (ENP), South Indian Ocean (SI), South Pacific (SP), Northern Hemisphere (NH; i.e., WNP + NA + ENP), Southern Hemisphere (SH; i.e., SI + SP), and the globe (All; i.e., NH + SH). Reproduced from Fig. 1 of Chan and Chan (2015). © International Journal of Climatology published by John Wiley & Sons Ltd on behalf of the Royal Meteorological Society.

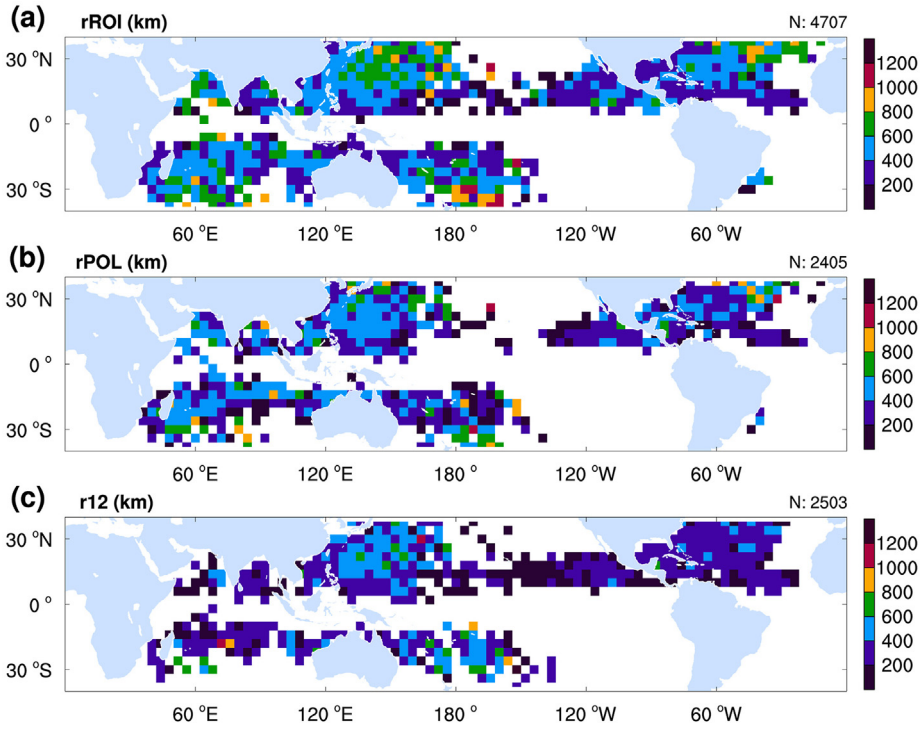

Fig. 2. Global TC size (km) distribution of the average SST cold wake size determined by the (a) Region of Interest (ROI) method (i.e., image processing algorithm), (b) POLAR method (i.e., assumes axisymmetric cold wake), and (c) r12 from scatterometer data (i.e., QuikSCAT-R) for a 4° latitude grid × 4° longitude grid. Sample sizes are denoted in the top right of each panel. Reproduced from Fig. 2 of Zhang et al. (2019).

square errors below the Best Track (Combot et al., 2020; Zhang et al., 2021). Application of new object-based approaches to this radar data may eventually be useful for quantifying the detailed characteristics (e.g., shape, symmetry) of outer winds (Matyas et al., 2018; Zick et al., 2022).

c) New advances in the factors impacting TC outer size and structure

i) Theory and idealized simulations

Recent work has identified new factors impacting TC outer wind field expansion following genesis. The TC expansion rate depends on its initial size in observations and simulations, with initially larger storms expanding more quickly (Xu and Wang 2010; Martinez et al., 2020). On the *f*-plane, this expansion rate depends strongly on initial size with a weak dependence on midtropospheric ambient moisture (Fig. 3; Martinez et al., 2020) providing context to earlier work (Hill and Lackmann 2009). The outer size growth rate is also sensitive to more complex factors such as cloud radiative forcing and boundary layer mixing (Bu et al., 2017; Bryan and Rotunno, 2009).

Moreover, recent work has developed a model for expansion that ultimately depends on the quantity of absolute angular momentum imports by the inflow velocity (Wang and Toumi, 2022). However, simulated TCs do not expand forever. Instead, they expand toward an equilibrium upper-bound size, called the "potential size" (Wang et al., 2022). Potential size scales approximately with the length-scale Vp/f, where Vp is the potential intensity and f is the Coriolis parameter (Chavas and Emanuel 2014). A similar $1/f$ scaling also occurs in idealized simulations including those without moisture (Cronin and Chavas 2019; Held and Zhao 2008).

In simulations on a rotating sphere, TC outer size in the tropics is strongly influenced by the Rhines scale, which is inversely dependent on β (i.e., rather than f) and governs the transition between waves and vortices in turbulent flow (Rhines 1975; Chavas and Reed 2019). This length scale increases slowly with latitude in the tropics, consistent with observations, reanalyses, and simulations (Chan and Chan 2015; Schenkel et al., 2023). Experiments varying planetary rotation rate and planetary radius showed that TCs were larger on bigger and/or slower-rotating planets, with changes among simulations scaling with the Rhines scale (Chavas and Reed 2019). Lu and Chavas (2022) confirmed these findings in a barotropic beta-plane model, showing that Rossby wave radiation weakens the vortex outer wind field, with faster-shrinking rates for larger vortices. Together, these simulations and theories have helped increase confidence in which, if any, external factors discussed below impact the storm outer size life cycle.

ii) Environmental factors

Recent work has identified a growing list of environmental factors that impact TC outer size and structure, whose relative importance has not been quantified. Specifically, Wang and Toumi, 2019 showed that dry midtropospheric air can broaden the TC wind field by enhancing the outer transverse circulation and its associated angular momentum imports, which provides nuance to prior studies (Hill and Lackmann,

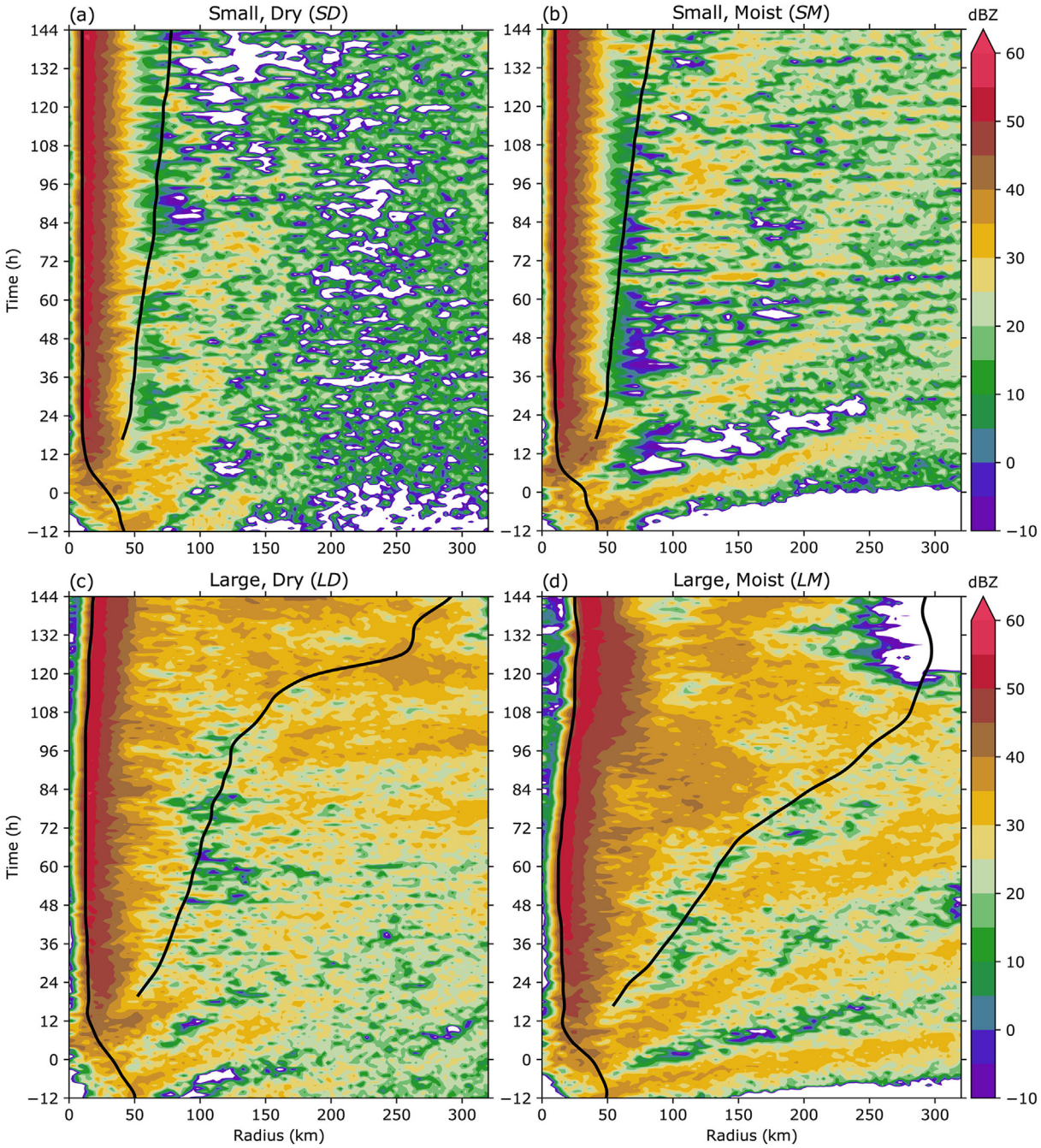

Fig. 3. Radar reflectivity (dBZ) at a 2-km altitude is shown as a function of TC-relative radius and time relative to the initiation of rapid intensification for the 3-D simulations: (a) Small, Dry (initial vortex), (b) Small, Moist, (c) Large, Dry, and (d) Large, Moist. The innermost black curve in each panel is the radius of maximum tangential winds and the outermost black curve is the radius of 34-kt tangential winds. Reproduced from Fig. 7 of Martinez et al. (2020).

2009; Martinez et al., 2020). Increased focus on the role of 850–200-hPa ambient vertical wind shear has shown a broadening of outer winds and convection in the downshear half of the storm (Zhou et al., 2018; Finocchio and Rios-Berrios, 2021). However, Yang et al. (2022) suggest that axisymmetric TC outer size may decrease despite this asymmetric expansion in the downshear half. The direction of the ambient lower-tropospheric flow relative to the vertical wind shear vector may be particularly important in determining whether the TC will change in intensity or outer size (Chen et al., 2018; 2019; 2021). TCs tend to expand most strongly when the ambient lower-tropospheric flow vector is pointed towards the upshear right quadrant, which leads to enhanced radial fluxes of vorticity and enthalpy into the outer rainbands (Rappin and Nolan 2012; Chen et al., 2019; 2021).

Several other disparate factors can also influence TC outer size and structure. Idealized aquaplanet simulations show that the magnitude and radius of outer precipitation increase for warmer SSTs, whereas the TC outer wind field size does not substantially change (Stansfield and Reed 2021; Wang and

Toumi 2018b). Instead, TC outer wind field size is sensitive to the magnitude of local SSTs relative to large-scale values (i.e., relative SSTs; Yang et al., 2022; Bruneau et al., 2020). Aside from SSTs, idealized simulations suggested the importance of tropospheric lapse rates compared to either ambient humidity or winds in impacting TC outer size (Ma et al., 2019). Finally, the TC diurnal cycle is also associated with periodic changes in TC outer storm structure with the strongest outer winds and convection occurring during the afternoon local time (Ditchek et al., 2019; Zhang et al., 2020). These factors add to the growing list of parameters previously shown to influence TC outer size.

iii) Landfall

Recent studies have used limited-area idealized modeling to examine the response of the TC outer wind field to landfall. Axisymmetric experiments in which the ocean surface is instantaneously changed to a rougher/drier land-like surface show that TC outer size decreases monotonically and rapidly after landfall, especially for a rough surface, with more gradual decreases for a dry surface (Chen and Chavas 2020; 2021). Using these simulations, recent work has shown that existing theory developed for the axisymmetric TC tangential wind field structure over the ocean can also predict the wind field response to landfall (Chen and Chavas 2023). Idealized three-dimensional experiments with a landfalling mature TC also show that outer size decreases monotonically, especially for a rougher surface (Hlywiak and Nolan 2021). This wind field response is highly asymmetric due to the frictional gradient between ocean and land (Hlywiak and Nolan 2022), with the front and front-left quadrants relative to TC motion decaying the fastest (Fig. 4) matching observations of Hurricane Harvey (Alford et al., 2019; Hlywiak and Nolan 2022). The landfall response of TC rainfall is also highly asymmetric with dependence on both vertical wind shear and land-ocean interactions (Zhou et al., 2018). In combination, this new bed of research offers hope for using models to better understand and predict the inland decay of hurricanes and their hazards.

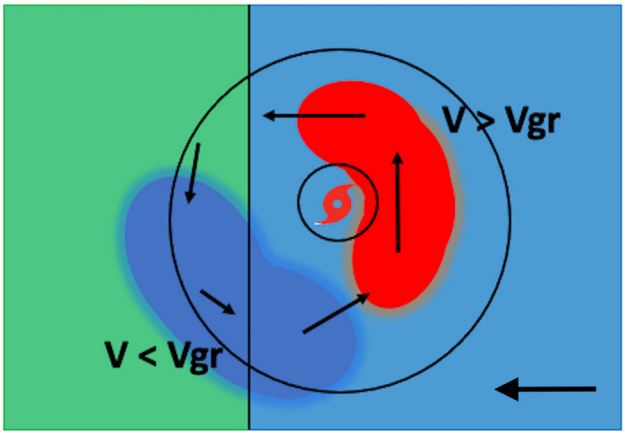

Fig. 4. Simple schematic illustrating the enhanced offshore inflow and acceleration of tangential winds behind the TC. The inner and outer wind fields are represented by the small circle and larger oval, respectively, with the western portion over land. The oval is skewed toward the offshore side to represent the expansion of the tropical storm force wind area. The large black arrow in the bottom-right corner shows the TC motion vector. Black arrows around the TC indicate the magnitude and direction of storm winds. The blue area represents the region of large inflow angles and subgradient winds, while the red area represents the supergradient winds at the boundary layer top. Reproduced from Fig. 23 of Hlywiak and Nolan (2022). © American Meteorological Society. Used with permission.

3. Progress in forecasting TC outer size and structure

a) Summary of historical operational practices

Operational TC outer size metrics are typically measured as R34, R50, and R64 (or equivalent radii) in four compass quadrants (i.e., northeast, southeast, southwest, northwest) and as the ROCI at some operational centers (Knaff et al., 2021). The 34-kt wind threshold is particularly important as it represents speeds where preparations for landfalling TCs become too dangerous or difficult (NHC 2017). Wind radii are routinely provided in operational products for the analysis position, but warning centers vary in the provision of radii for forecast positions. Depending on the warning center, a full wind structure analysis and forecast for an intense and long-lived TC can require multiple wind radii assessments for the analysis and all forecast points along the track. TC outer size analyses and forecasts use both observations (e.g., scatterometers) and numerical weather prediction (NWP) output. These analyses and forecasts are typically skillful compared to a wind radii climatology and persistence (CLIPER) model (Landsea and Franklin 2013; Sampson et al., 2018). ROCI analyses and forecasts are particularly prone to larger errors due to enhanced subjectivity in constructing estimates, the sparsity of available nearby surface pressure observations, and the sensitivity to the methods and tools employed to analyze the pressure field (Knaff et al., 2014). The R34 and R64 estimates are triggers for cyclone watches and warnings, which motivates their importance.

b) Comparison of practices among operational centers

i) Overview

Most operational center analysis techniques for assessing wind radii rely heavily on satellite-based estimates of ocean surface winds [e.g., Advanced Scatterometer (ASCAT)] given their excellent spatial coverage, and reliable accuracy and precision (Chou et al., 2013; Stiles and Coauthors, 2014). While some operational centers may ingest ocean surface wind fields directly into guidance or production analysis tools, there is a heavy reliance on "third-party" providers for the presentation of these data via publicly available websites (e.g., NESDIS/NOAA Center for Satellite Application and Research, https://manati.star.nesdis.noaa.gov/index.php). If there is no available observed wind speed imagery or in-situ observations, forecasters will use NWP guidance blended with surface observations and partial wind speed images while accounting for any NWP biases (Cangialosi and Landsea 2016; Sampson et al., 2018).

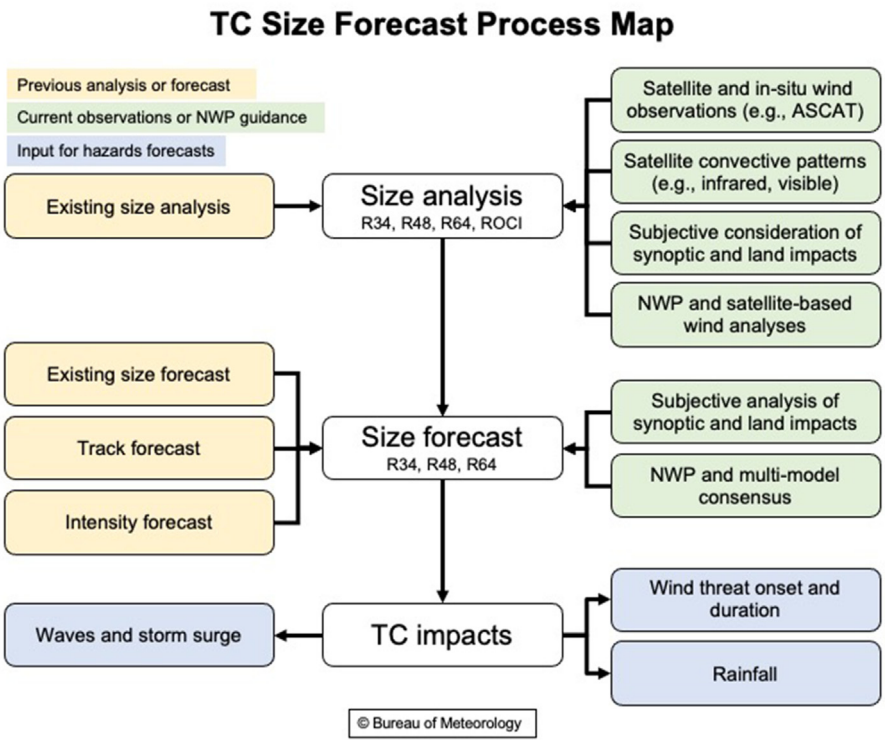

Fig. 5. BoM forecast process for TC size parameters. Figure courtesy of Joe Courtney (BoM).

As an example of the specific data and methods, Fig. 5 from the Bureau of Meteorology (BoM) shows that the size analysis is a subjective process that incorporates new information into the prior size analysis (when available) including: surface observations, satellite winds, NWP surface winds, changes in synoptic influences and land proximity, and changes in convective patterns from geostationary satellites (Landsea and Franklin 2013; Knaff et al., 2021). The NOAA/NESDIS CIRA TC wind analysis (i.e., synthesis of satellite and in situ data) is also used to make analyses at some operational centers, but less so in making forecasts (Knaff et al., 2011).

TC outer size forecasting is a subjective process that uses the prior forecast (when available) together with the latest information including the most recent analysis with a strong dependence on NWP forecasts of TC structure, intensity, track, and the synoptic-scale environment (e.g., monsoon flow) as summarized in Fig. 5 (Sampson et al., 2018). Both deterministic and ensemble global and mesoscale models have been shown to produce skillful forecasts of R34 (Cangialosi and Landsea 2016; Bachmann and Torn 2021). Comparisons of model output during the forecast process are done subjectively, while objective guidance (i.e., NWP wind radii consensus) can also be considered where available at operational centers. However, forecaster input is crucial given the bias towards small TCs inherent to NWP (Knaff and Sampson 2015; Cangialosi and Landsea 2016). Both the National Hurricane Center (NHC) and JWTC also consider output from CLIPER, which is competitive with NWP output (Knaff et al. 2007; 2018). Using these tools, verification shows that both NHC and JWTC TC outer size forecasts and analyses are skillful relative to CLIPER at all lead times (Cangialosi and Landsea 2016; Sampson et al., 2017).

There exists considerable variability in the format of R34, R50, and R64 (or equivalent radii) analyses and forecasts among agencies given the lack of a global standard. Examples of ocean wind warnings containing wind radii from the BoM and Joint Typhoon Warning Center (JTWC) are provided in Tables A.1 and A.2, respectively. While most centers provide outer wind products (e.g., R34), fewer centers provide ROCI, which may instead be used internally as part of operational procedures to assess TC outer size. An example of how ROCI is listed in a Technical Bulletin (alongside wind radii) from the BoM in an example in Table A.3. Only the NHC and JWTC perform post-season analyses of operational R34 and ROCI forecasts to address real-time forecasting errors like the example to be shown in the next subsection.

The graphical presentation of the TC outer size wind quadrants is equally varied among operational centers with some choosing to not show graphical products. The differences in those forecasting centers that provide graphics are partially due to the use of different software packages. These graphics, in the form of TC forecast track maps, are used to help explain the current location and forecast track of the cyclone to both decision-makers and the general public. For example, JTWC, NHC, and Central Pacific Hurricane Center (CPHC) use the Automated Tropical Cyclone Forecast (Sampson and Schrader 2000) platform, which is used to overlay and manually adjust wind radii analyses over the wind speed graphics provided by Naval Research Laboratory (NRL) that serve as a first guess (Cangialosi and Landsea 2016; Sampson et al., 2017). In

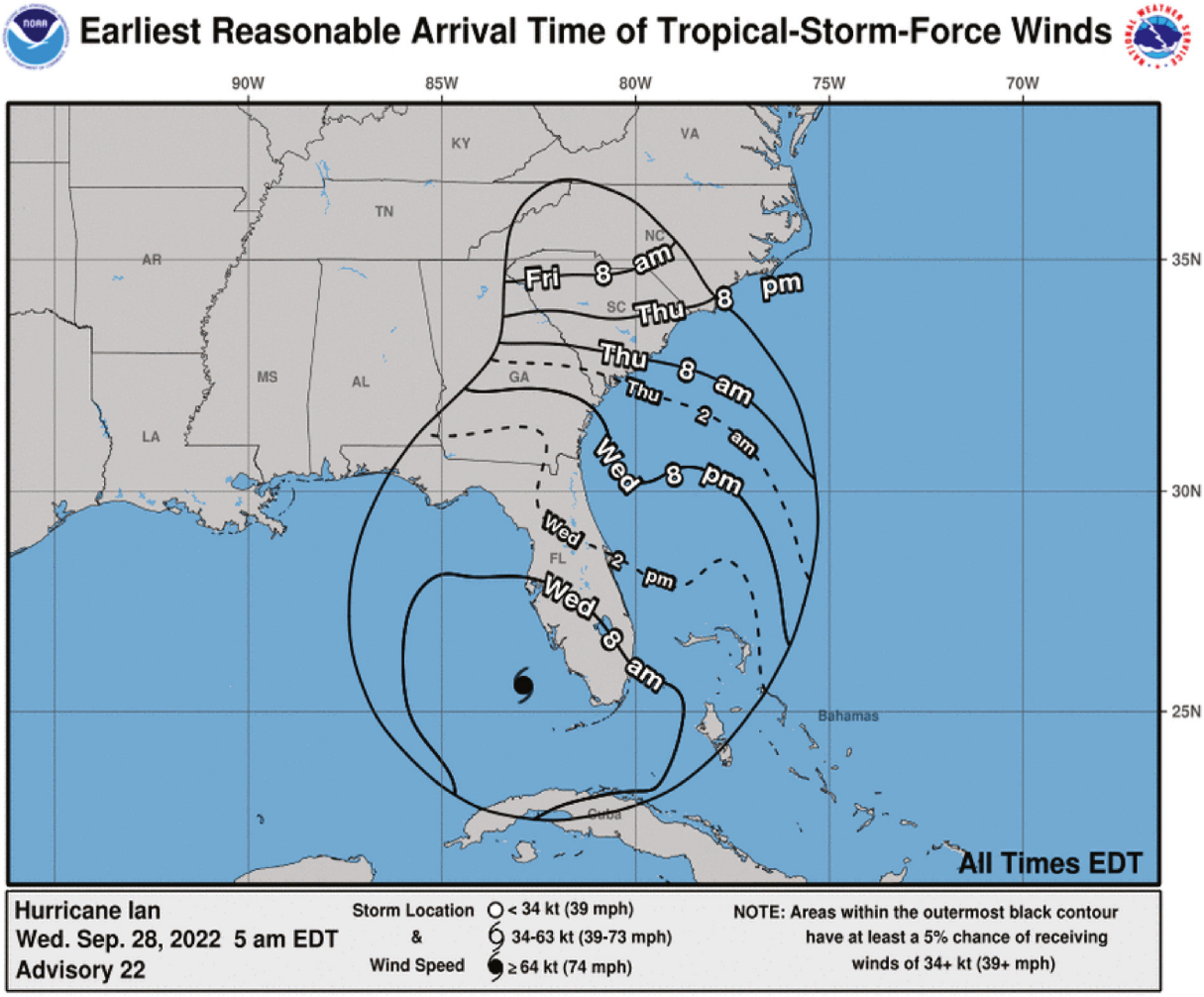

Fig. 6. Example of wind arrival time graphic (contours) from the NHC showing the earliest reasonable arrival time of 34-kt winds for Hurricane Ian on 28 Sep 2022. Figure courtesy of the NHC.

contrast, Tropical Cyclone Warning Center (TCWC) Melbourne, RSMC Nadi, TCWC Jakarta, and other South Pacific national warning centers all use the "TC Module" developed by the BoM. Selected examples of cyclone warning graphics with the forecasted wind fields are shown in Figs. A.1, A.2, and A.3 from Regional Specialized Meteorological Center (RSMC) Nadi, Tropical Cyclone Warning Center (TCWC) Wellington, and NHC, respectively. For RSMC La Reunion and New Delhi, both centers provide the radial extent of 28-kt winds (R28) in the four quadrants of the TC in addition to R34 information (IMD 2021). In contrast to other operational centers, the Japanese Meteorological Agency (JMA) provides the radius of 30-kt winds (R30) rather than R34, depicting these as circles rather than quadrants in their graphical warning map (JMA, 2022). If the wind field distribution is concentric, the center of the wind radii circle will coincide with the TC center in their analyses and forecasts. In cases of outer wind field asymmetries, the R30 wind radii circle will be offset from the storm center with the values quoted in the text product more simply as radii in two semi-circles rather than in quadrants as shown in Fig. A.4 (JMA, 2022).

Recent innovations have focused on developing products that better serve end users. One product that does provide additional information to aid decision-making is the wind arrival time map published by the NHC. Two versions of the map show the "earliest reasonable arrival time" (Fig. 6) or the "most likely arrival time" of tropical storm-force winds, which are crucial for use by emergency managers to determine when preparations should be completed (NHC 2017).

ii) Example analysis and forecast

Additional insight into the current state of operational forecasting is provided through a case study. During late August and early September 2022, Typhoon Hinnamnor (designated Super Typhoon 12W by JTWC) formed south of Japan and tracked west towards Taiwan before recurving to the north over the East China Sea and South Korea. On its first approach to Okinawa, a sequence of satellite-derived wind speed images (Fig. 7) provided an accurate depiction of its compact, atypical wind field, allowing a smaller gale extent to be forecast and, thus, preventing costly protective preparations

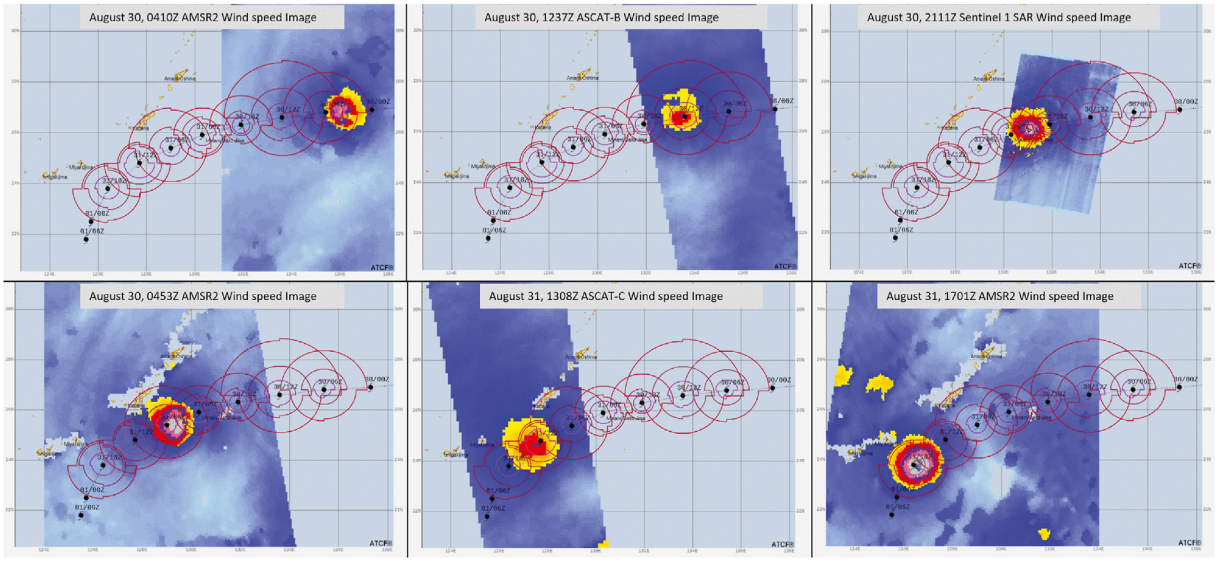

Fig. 7. R34, R50, and R64 wind analyses (contours) of Super Typhoon 12W on approach to Okinawa, Japan from 30 August 2022 to 31 August 2022, with wind speed overlaid (kt; shading). Note the along-track variation in analysis size suggesting an inconsistent adjustment of the analyses from objective best rack wind radii guidance. Figure courtesy of Stephen Barlow (JWTC).

on the island. Despite the relative accuracy of the forecasts, the objectively weighted best track wind radii guidance (i.e., OBTK), which uses satellite and climatological size data, depicted a larger than observed wind field leading to inconsistent sizes among sequential analysis times issued by forecasters. This example highlights a need for further training on the use of the forecast products (Sampson et al., 2017; 2018). As Super Typhoon 12W stalled southwest of Okinawa, the wind structure expanded rapidly (Fig. A.6) after absorbing the remnants of Tropical Depression 13W, leading to gale-force winds impacting regions as far as Taiwan. During these track and structure changes, both the wind radii consensus model and objectively weighted best track wind radii guidance accurately depicted the evolving wind field, as well as throughout the life cycle of Super Typhoon 12W (Fig. 7 and A.6). These skillful forecasts facilitated efficient and timely preparations to be made ahead of the second passage past Okinawa as Super Typhoon 12W moved north. Post-storm analysis adjusted wind radii for consistency based on a reexamination of the wind speed images and surface observations (Figs. A.5 and A.6).

c) New operational developments

Incremental improvements have been made to analyses and forecasts of TC outer size and structure since 2018. Operational centers are utilizing an increasing number of near real-time wind speed images to better refine wind radii analyses (e.g., ASCAT). Surface wind graphics from the satellite-based Compact Ocean Wind Vector Radiometer (Brown et al., 2017) will also be available soon, providing both crucial surface wind field and moisture data after the recent loss of ASCAT-A data. In the absence of satellite data and in situ observations, the availability of R34 output for TCs from the European Centers for Medium-Range Weather Forecasts (ECMWF) deterministic model, beginning in June 2020, has been important for all operational centers.

JTWC implemented manual post-storm quality control of 34-kt wind radii for western North Pacific tropical cyclones beginning with the 2016 season and all basins starting with the 2019 season. Presently, personnel at the NHC, CPHC, BoM, and JTWC conduct post-season review of operational R34, R50, and R64 analyses resolving the types of inconsistencies in real-time analysis data highlighted in Fig. 7. NHC, CPHC, and BoM also conduct post-season reviews of ROCI data. All quadrant wind radii data from RSMC La Reunion as well as R30 and R50 short and long axis distance and direction from RSMC Tokyo are also available in best track data archives from both centers.

Several operational centers have also implemented new forecasting tools or provided additional forecast output. In 2021, a Markov-like (i.e., the future state is dependent on the past state) CLIPER model to forecast TC wind radii along the JTWC forecast track was integrated into the Automated Tropical Cyclone Forecast. This model, developed by NRL and NOAA National Environmental Satellite Data and Information Service (NESDIS), uses satellite-only estimates of TC outer size, which are statistically combined with intensity and motion forecasts to produce R34 forecasts. This model makes wind radii forecasts that are more consistent with initial storm sizes reducing the biases of the original CLIPER-derived wind radii at longer lead times, which are relaxed towards climatology.

Another innovation is the addition of forecasted TC position, intensity, and R34 data at 60 h, beginning in 2020, by the NHC in their operational warning products. This additional forecast time meant that NHC is now providing R34 forecasts at 12-h intervals through 72 h. Rather than providing just TC intensity and size radii, NHC is also testing a gridded two-

dimensional surface wind field, called the Wind Speed Probability Model Tropical Cyclone Message. The two-dimensional wind field is constructed using a Rankine vortex and wavenumber one asymmetry associated with storm motion using TC intensity and outer size data input from NHC analyses and forecasts together with NWP guidance (DeMaria et al., 2020; Santos et al., 2021).

Since December 2020, RSMC La Reunion has produced 5-day wind radii forecasts in official warnings derived from a statistical-dynamical model (T. Krait, personal communication, September 9, 2022). This model uses forecasts of equivalent TC wind radii derived from the ECMWF Integrated Forecast System and the National Centers for Environmental Prediction (NCEP) Global Forecast System as predictors to statistically derive R28, R34, R48, and R64 that are checked by forecasters for consistency. This model has shown skill increases exceeding 20% relative to raw ECMWF Integrated Forecast System wind radii forecasts. Together, these new data and techniques have yielded progress in TC outer size and structure analysis and forecasting.

4. TC outer circulation size and structure changes in the 21st century

a) Trends during the satellite era

No significant trends in TC outer wind field size have been shown for the satellite era (i.e., ~1979–present) according to reanalyses (Mok et al., 2018; Zhang and Chan 2023), modeling (Kreussler et al., 2021), and SST cold wake widths (Zhang et al., 2019; Wang and Toumi, 2021). Specifically, these datasets show that high-frequency variability dominates any low-frequency variability except in the South Indian Ocean as shown in Fig. 8 (Schenkel et al., 2017; Mok et al., 2018; Yang et al., 2022; Zhang and Chan 2023). Together, the strong agreement among these disparate datasets increases confidence in concluding that current climate trends are absent. However, some of these storm outer size datasets contain nontrivial uncertainty that may be larger than any decadal trends suggesting that these are lower-confidence conclusions.

b) Projected late 21st-century changes in TC outer size and structure

i) TC wind field

Current consensus shows differing conclusions among projections of TC outer wind versus precipitation changes by the late 21st century. This is despite previous studies showing that TC outer wind and precipitation size metrics are typically strongly correlated under current climate conditions, with most precipitation typically inwards of these metrics (Matyas 2010; Chavas et al., 2016). Beginning with the TC wind field, most research suggests that there will be no global changes in the life cycle of outer size and structure by the late 21st century despite significant changes in TC intensity and track. However, the absence of complete consensus suggests limited confidence in this conclusion. Specifically, global model simulations forced with different anthropogenic climate change scenarios [i.e., Coupled Model Intercomparison Project phase 3 (CMIP3) and phase 6 (CMIP6)] have shown either: 1) variability in the sign and magnitude of TC outer size change among basins or 2) no global changes in TC outer winds (Yamada et al., 2017; Kreussler et al., 2021). This large inter-basin variability in TC outer size changes among basins, in particular, is consistent with earlier downscaled regional model simulations of global TC activity, which suggests that the impact of internal climate variability (e.g., El Niño-Southern Oscillation) on TC outer size may be dominant over greenhouse gas forcing (Knutson et al., 2015). Additionally, pseudo-global warming regional model simulations of three intense landfalling Australian TCs by Parker et al. (2018) also showed no projected changes in TC outer size and structure, despite significant changes in track and intensity under CMIP5 perturbations. In contrast to these single model studies using single climate change scenarios, Schenkel et al. (2023) focused on North Atlantic TC outer size and structure using multiple regional and global coupled models under two different climate warming scenarios (i.e., CMIP5 and CMIP3). This study also included initial and boundary conditions with and without current climate variability. This study showed no projected changes in the life cycle of TC outer size and structure, including at genesis and lifetime maximum values, by the late 21st century as shown in Fig. 9. These conclusions also more broadly agree with idealized aquaplanet simulations that show no changes in storm outer wind field size with increasing SSTs (Stansfield and Reed 2021).

In contrast to these aforementioned studies, Stansfield et al. (2020) projected 10–20% increases in North Atlantic TC outer size by the late 21st century using global model ensemble simulations under CMIP5 perturbations. The magnitude of these increases matches global simulations by Kim et al. (2014), which used a much stronger climate change scenario with doubled CO_2. However, these projected outer size increases also match the magnitude of nonsignificant changes within select simulations from prior work suggesting sensitivity to sample size and the statistical testing method used (Schenkel et al., 2023; Knutson et al., 2015). In combination, the projected global changes in TC outer wind field size and structure by the late 21st century vary from no change to a 20% increase relative to the current climate, with most studies on the lower end of this range.

ii) TC precipitation

Compared to TC outer winds, there are fewer studies and less consensus on whether outer precipitation will change by the late 21st century. In particular, Knutson et al. (2015) projected increased TC precipitation rates at all radii within 500 km of the TC center in nearly all global basins. These increases were similar to the expected increases of 7% per °C from the Clausius-Clapeyron equation (Knutson et al., 2015; Stansfield and Reed 2021). In contrast, Yamada et al. (2017) projected no changes in TC outer precipitation rate in all basins, despite showing variability in the sign and magnitude of outer wind field size changes among basins. Patricola and

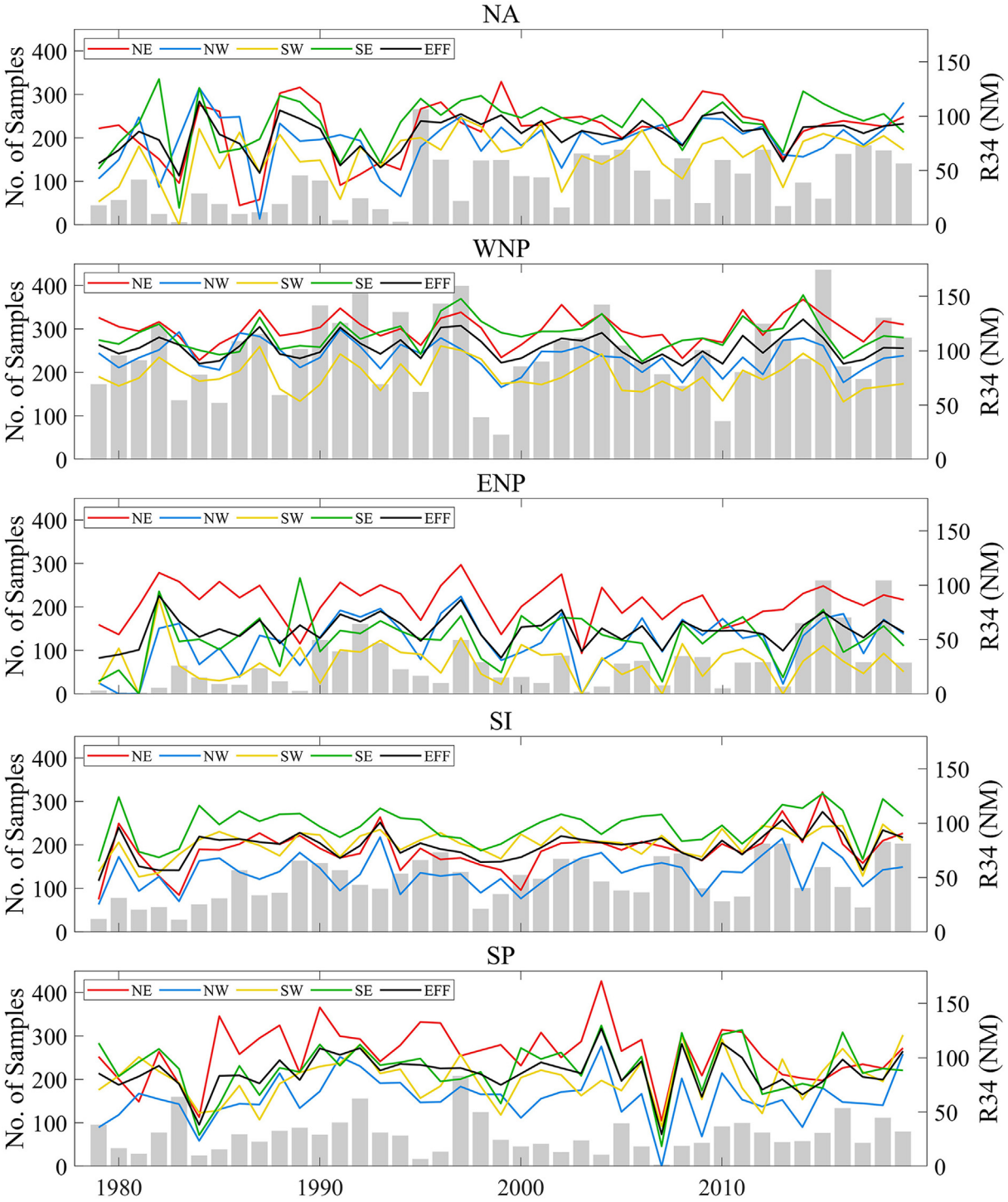

Fig. 8. Time series of annual mean R34 in four quadrants and R34EFF (mean of quadrants) for five basins (NA: North Atlantic; WNP: western North Pacific; ENP: eastern North Pacific; SI: South Indian Ocean; SP: South Pacific) in 1979–2019 calculated from the ECMWF fifth-generation reanalysis (ERA5). The bars indicate the corresponding number of samples. Reproduced from Fig. 3 of Zhang and Chan (2023). © International Journal of Climatology published by John Wiley & Sons Ltd on behalf of Royal Meteorological Society.

Wehner (2018) projected that the outer extent and magnitude of precipitation would either remain unchanged or decrease with increasing anthropogenic warming using pseudo-global warming hindcasts of 15 intense TCs under CMIP5 perturbations. Finally, idealized simulations showed increases in the horizontal extent and magnitude of outer precipitation rates with uniform warming of SSTs (Stansfield and Reed 2021). These few studies and their diverse set of responses warrant further research especially given their differences with the TC outer wind field results, since outer precipitation and wind field sizes tend to be strongly correlated (Matyas 2010; Reed and Chavas 2015; Chavas et al., 2016).

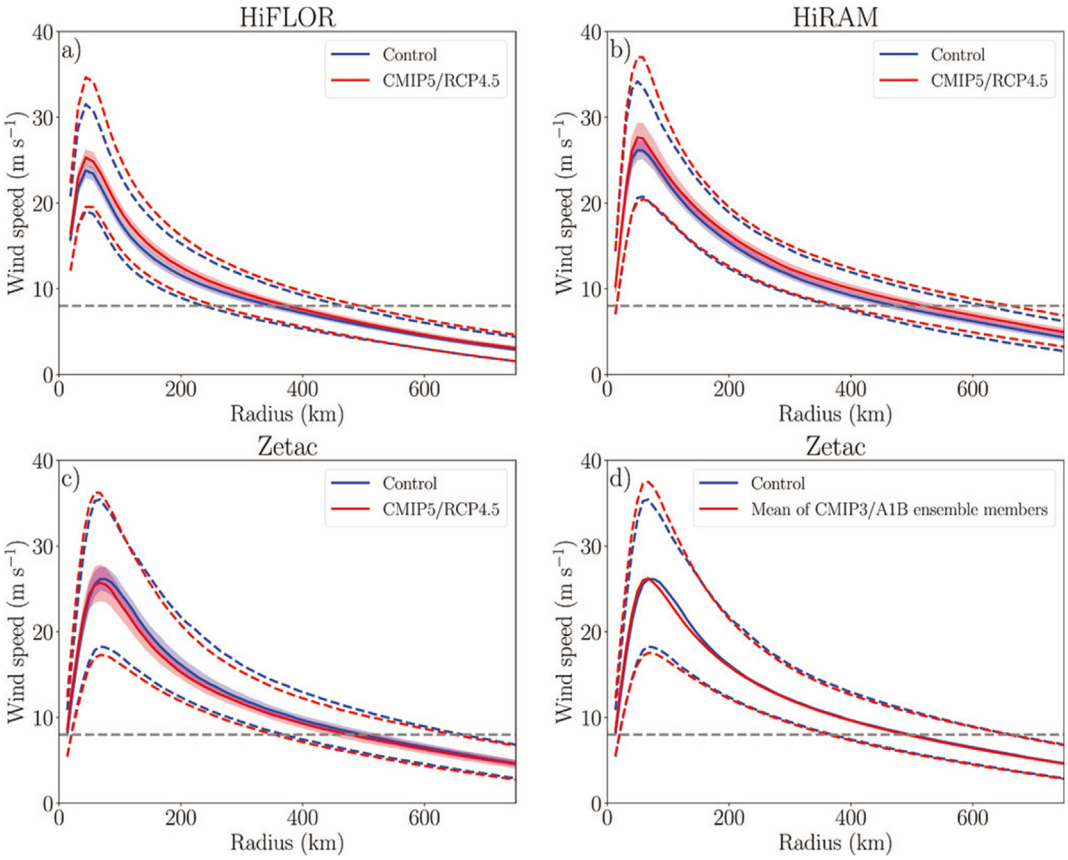

Fig. 9. Radial profile of composite median (solid line) with its 95% confidence interval (shaded) calculated using a 1000 sample bootstrap approach, and the interquartile range (dashed lines) of the azimuthal-mean 10-m azimuthal wind (m s^{-1}) for the control, and late 21st-century simulations in (a) HiFLOR (global model), (b) HiRAM-downscaling GFDL hurricane model (regional model), and (c) Zetac-downscaling GFDL hurricane model (regional model) from the CMIP5/RCP4.5 simulation, and (d) the Zetac-downscaling GFDL hurricane model (regional model) from All 10 CMIP3/A1B ensemble members (excluding the ensemble mean). The downscaling of the global and regional model data serves as initial and boundary conditions for the GFDL hurricane model. None of the radii show significant differences in median values between the current and late 21st-century climate for a false discovery rate of $\alpha = 0.1$ or $\alpha = 0.2$. In panel (d), ≥80% of the 10 ZETAC-downscaling CMIP3/A1B ensemble members show no change in azimuthal wind speeds at all radii. Reproduced from Fig. 2 of Schenkel et al. (2023). © American Meteorological Society. Used with permission.

c) Factors impacting projected TC outer size changes

There remains an incomplete understanding of which factors are responsible for the projected changes, or the lack thereof, in TC outer size and structure. This is partially attributable to the large number of factors discussed earlier that influence TC outer size and structure, whose relative importance has yet to be quantified. Despite these uncertainties, the Rhines scaling is likely particularly important to understanding projected changes in TC outer winds given its relevance to observations and theory (Chavas and Reed 2019; Schenkel et al., 2023). The shrinking process associated with the Rhines scaling is largely dependent on the meridional gradient of planetary vorticity and, hence, is thermodynamically invariant (Chavas and Reed, 2019; Schenkel et al., 2023). Expectations from the Rhines scaling suggest no global changes in outer wind field size consistent with simulations using a broad range of SSTs (Stansfield and Reed 2021) and a diverse set of climate change scenarios (Schenkel et al., 2023; Yamada et al., 2017). Nonetheless, additional work is needed to comprehensively identify the most important factors in the current climate and to understand how these factors change as the climate warms.

5. Summary and discussion

Continued progress has been made in our understanding and ability to research and forecast the outer size and structure of TC winds and precipitation. The quality of TC outer size and structure datasets have continued to improve since IWTC-9. Furthermore, there is a more complete understanding of the outer size life cycle through the identification of additional factors impacting the outer region of the storm. Moreover, forecasts of TC outer size have become more skillful due to an increasing quantity of satellite observations, although procedures and products (including reliance on third-party visualizations) remain highly varied among operational centers. Detailed, manual post-season review of R34 (as well as R50 and R64) by operational centers is increasing, particularly with the pending expansion of JTWC post-season reviews to Indian Ocean and Southern Hemisphere cyclones. Conducting post-storm quality control of all quadrant wind radii for inclusion in final best track

datasets should remain a high priority as these data support the development and improvement of impact-based forecast and warning services for decision makers. Finally, most late 21st-century projections suggest no global changes in TC outer winds throughout the TC life cycle matching current climate trends, whereas changes in TC outer precipitation remain more uncertain despite its strong relationship with the storm outer wind field. However, additional work is needed to identify which factors most strongly impact TC outer winds and, especially, precipitation to better anticipate any future changes. From this review of research and operations, our highest priority recommendation is the continued launch of satellites that observe the entire life cycle of TC outer winds and precipitation to improve forecasts and our understanding of the evolution of these fields.

Acknowledgments

We would like to thank the topic co-chairs, Elizabeth Ritchie (Monash) and Matthew Kucas (JTWC), and the workshop organizers, Joe Courtney (BoM) and Rob Rogers (HRD), for the opportunity to write this review article and for their guidance and feedback. The authors would like to thank two anonymous reviewers, Kim Hoogewind (CIWRO/NSSL), and Dongliang Wang (CMA) for constructive feedback. We would also like to thank representatives from RSMC La Reunion and the BoM for their input. Finally, we thank the World Meteorological Organization's World Weather Research Program and Tropical Cyclone Program for supporting the activities of this working group. Ben Schenkel was supported by funding from NOAA/Office of Oceanic and Atmospheric Research under NOAA-University of Oklahoma Cooperative Agreement #NA21OAR4320204, U.S. Department of Commerce, and NSF AGS #2028151. Daniel Chavas is supported by NSF AGS #1945113. Kelvin T. F. Chan was jointly supported by the National Science Foundation, United States, National Key R&D Program of China (2019YFC1510400), the National Natural Science Foundation of China (41975052), the Guangdong Basic and Applied Basic Research Foundation (2023A1515010741), the Innovation Group Project of the Southern Marine Science and Engineering Guangdong Laboratory (Zhuhai; 311021001), and the Guangdong Province Key Laboratory for Climate Change and Natural Disaster Studies (2020B1212060025).

Appendix A. Supplementary data

Supplementary data to this article can be found online at https://doi.org/10.1016/j.tcrr.2023.09.002.

References

Alford, A.A., Biggerstaff, M.I., Carrie, G.D., Schroeder, J.L., Hirth, B.D., Waugh, S.M., 2019. Near-surface maximum winds during the landfall of Hurricane Harvey. Geophys. Res. Lett. 46, 973–982. https://doi.org/10.1029/2018GL080013.

Bachmann, K., Torn, R.D., 2021. Validation of HWRF-based probabilistic TC wind and precipitation forecasts. Wea. Forecast. 36, 2057–2070. https://doi.org/10.1175/WAF-D-21-0070.1.

Bian, G.-F., Nie, G.-Z., Qiu, X., 2021. How well is outer tropical cyclone size represented in the ERA-5 reanalysis dataset? Atmos. Res. 249, 105–339. https://doi.org/10.1016/j.atmosres.2020.105339.

Brown, S., Focardi, P., Kitiyakara, A., Maiwald, F., Milligan, L., Montes, O., Padmanabhan, S., Redick, R., Russel, D., Bach, V., Walkemeyer, P., 2017. The COWVR Mission: demonstrating the capability of a new generation of small satellite weather sensors. In: 2017 IEEE Aerospace Conference. IEEE, Big Sky, MT, USA, p. 1e7. https://doi.org/10.1109/AERO.2017.7943884.

Bruneau, N., Wang, S., Toumi, R., 2020. Long memory impact of ocean mesoscale temperature anomalies on tropical cyclone size. Geophys. Res. Lett. 47, e2019GL086165. https://doi.org/10.1029/2019GL086165.

Bryan, G.H., Rotunno, R., 2009. The maximum intensity of tropical cyclones in axisymmetric numerical model simulations. Mon. Wea. Rev. 137, 1770–1789. https://doi.org/10.1175/2008MWR2709.1.

Bu, Y.P., Fovell, R.G., Corbosiero, K.L., 2017. The influences of boundary layer mixing and cloud-radiative forcing on tropical cyclone size. J. Atmos. Sci. 74, 1273–1292. https://doi.org/10.1175/JAS-D-16-0231.1.

Cangialosi, J.P., Landsea, C.W., 2016. An examination of model and official National Hurricane Center tropical cyclone size forecasts. Wea. Forecast. 31, 1293–1300. https://doi.org/10.1175/WAF-D-15-0158.1.

Chan, K.T.F., Chan, J.C.L., 2015. Global climatology of tropical cyclone size as inferred from QuikSCAT data. Int. J. Climatol. 35, 4843–4848. https://doi.org/10.1002/joc.4307.

Chan, K.T.F., Chan, J.C.L., 2018. The outer-core wind structure of tropical cyclones. J. Meteorol. Soc. Jpn. 96, 297–315. https://doi.org/10.2151/jmsj.2018-042.

Chavas, D.R., Emanuel, K., 2010. A QuikSCAT climatology of tropical cyclone size. Geophys. Res. Lett. 37, L18816. https://doi.org/10.1029/2010GL044558.

Chavas, D.R., Emanuel, K., 2014. Equilibrium tropical cyclone size in an idealized state of axisymmetric radiative–convective equilibrium. J. Atmos. Sci. 71, 1663–1680. https://doi.org/10.1175/JAS-D-13-0155.1.

Chavas, D.R., Reed, K.A., 2019. Dynamical aquaplanet experiments with uniform thermal forcing: system dynamics and implications for tropical cyclone genesis and size. J. Atmos. Sci. 76, 2257–2274. https://doi.org/10.1175/JAS-D-19-0001.1.

Chavas, D.R., Lin, N., Emanuel, K., 2015. A model for the complete radial structure of the tropical cyclone wind field. Part I: comparison with observed structure. J. Atmos. Sci. 72, 3647–3662. https://doi.org/10.1175/JAS-D-15-0014.1.

Chavas, D.R., Lin, N., Dong, W., Lin, Y., 2016. Observed tropical cyclone size revisited. J. Clim. 29, 2923–2939. https://doi.org/10.1175/JCLI-D-15-0731.1.

Chen, J., Chavas, D.R., 2020. The transient responses of an axisymmetric tropical cyclone to instantaneous surface roughening and drying. J. Atmos. Sci. 77, 2807–2834. https://doi.org/10.1175/JAS-D-19-0320.1.

Chen, J., Chavas, D.R., 2021. Can existing theory predict the response of tropical cyclone intensity to idealized landfall? J. Atmos. Sci. 78, 3281–3296. https://doi.org/10.1175/JAS-D-21-0037.1.

Chen, J., Chavas, D.R., 2023. A model for the tropical cyclone wind field response to idealized landfall. J. Atmos. Sci. 80, 1163–1176. https://doi.org/10.1175/JAS-D-22-0156.1.

Chen, B., Davis, C.A., Kuo, Y., 2018. Effects of low-level flow orientation and vertical shear on the structure and intensity of tropical cyclones. Mon. Wea. Rev. 146, 2447–2467. https://doi.org/10.1175/MWR-D-17-0379.1.

Chen, B., Davis, C.A., Kuo, Y., 2019. An idealized numerical study of shear-relative low-level mean glow on tropical cyclone intensity and size. J. Atmos. Sci. 76, 2309–2334. https://doi.org/10.1175/JAS-D-18-0315.1.

Chen, B., Davis, C.A., Kuo, Y., 2021. Examination of the combined effect of deep-layer vertical shear direction and lower-tropospheric mean flow on tropical cyclone intensity and size based on the ERA5 reanalysis. Mon. Wea. Rev. 149, 4057–4076. https://doi.org/10.1175/MWR-D-21-0120.1.

Chou, K.-H., Wu, C.C., Lin, S.-Z., 2013. Assessment of the ASCAT wind error characteristics by global dropwindsonde observations. J. Geophys. Res. Atmos. 118, 9011–9021. https://doi:10.1002/jgrd.50724.

Combot, C., Mouche, A., Knaff, J., Zhao, Y., Zhao, Y., Vinour, L., Quilfen, Y., Chapron, B., 2020. Extensive high-resolution synthetic aperture radar

(SAR) data analysis of tropical cyclones: comparisons with SFMR flights and Best Track. Mon. Wea. Rev. 148, 4545–4563. https://doi.org/10.1175/MWR-D-20-0005.1.

Cronin, T.W., Chavas, D.R., 2019. Dry and semidry tropical cyclones. J. Atmos. Sci. 76, 2193–2212. https://doi.org/10.1175/JAS-D-18-0357.1.

DeMaria, M., Santos Jr., P., Onderlinde, M., DeMaria, G., Ostwald, O., 2020. A gridded version of the National Hurricane Center official forecasts to support operations at national centers and weather forecast offices. Part I: model formulation. In: 100th AMS Annual Meeting, 1.2. Amer. Meteor. Soc., Boston, MA.

Demuth, J., DeMaria, M., Knaff, J., 2006. Improvement of advanced microwave sounding unit tropical cyclone intensity and size estimation algorithms. J. Appl. Meteorol. Climatol. 45, 1573–1581. https://doi.org/10.1175/JAM2429.1.

Ditchek, S.D., Molinari, J., Corbosiero, K.L., Fovell, R.G., 2019. An objective climatology of tropical cyclone diurnal pulses in the Atlantic basin. Mon. Wea. Rev. 147, 591–605. https://doi.org/10.1175/MWR-D-18-0368.1.

Emanuel, K., 2004. In: Federovich, E., Rotunno, R., Stevens, B. (Eds.), Tropical Cyclone Energetics and Structure. Atmospheric Turbulence and Mesoscale Meteorology. Cambridge University Press, pp. 165–192.

Finocchio, P.M., Rios-Berrios, R., 2021. The intensity-and size-dependent response of tropical cyclones to increasing vertical wind shear. J. Atmos. Sci. 78, 3673–3690. https://doi.org/10.1175/JAS-D-21-0126.1.

Held, I.M., Zhao, M., 2008. Horizontally homogeneous rotating radiative–convective equilibria at GCM resolution. J. Atmos. Sci. 65, 2003–2013. https://doi.org/10.1175/2007JAS2604.1.

Hill, K.A., Lackmann, G.M., 2009. Influence of environmental humidity on tropical cyclone size. Mon. Wea. Rev. 137, 3294–3315. https://doi.org/10.1175/2009MWR2679.1.

Hlywiak, J., Nolan, D.S., 2021. The response of the near-surface tropical cyclone wind field to inland surface roughness length and soil moisture content during and after landfall. J. Atmos. Sci. 78, 983–1000. https://doi.org/10.1175/JAS-D-20-0211.1.

Hlywiak, J., Nolan, D.S., 2022. The evolution of asymmetries in the tropical cyclone boundary layer wind field during landfall. Mon. Wea. Rev. 150, 529–549. https://doi.org/10.1175/MWR-D-21-0191.1.

IMD, 2021. Cyclone Warning in India Standard Operation Procedure [available online at. https://rsmcnewdelhi.imd.gov.in/uploads/report/61/61_245057_Cyclone%20Warning%20SOP%20Booklet%20final.pdf.

Irish, J.L., Resio, D.T., Ratcliff, J.J., 2008. The influence of storm size on hurricane surge. J. Phys. Oceanogr. 38, 2003–2013. https://doi.org/10.1175/2008JPO3727.1.

JMA, 2022. Notes on RSMC Tropical Cyclone Information [available online at: https://www.jma.go.jp/jma/jma-eng/jma-center/rsmc-hp-pub-eg/advisory.html.

Kim, H.-S., Vecchi, G.A., Knutson, T.R., Anderson, W.G., Delworth, T.L., Rosati, A., Zeng, F., Zhao, M., 2014. Tropical cyclone simulation and response to CO2 doubling in the GFDL CM2.5 high-resolution coupled climate model. J. Clim. 27, 8034–8054. https://doi.org/10.1175/JCLI-D-13-00475.1.

Knaff, J.A., Sampson, C.R., 2015. After a decade are Atlantic tropical cyclone gale force wind radii forecasts now skillful? Wea. Forecast. 30, 702–709. https://doi.org/10.1175/WAF-D-14-00149.1.

Knaff, J.A., Sampson, C.R., DeMaria, M., Marchok, T.P., Gross, J.M., McAdie, C.J., 2007. Statistical tropical cyclone wind radii prediction using climatology and persistence. Wea. Forecast. 22, 781–791. https://doi.org/10.1175/WAF1026.1.

Knaff, J.A., DeMaria, M., Molenar, D.A., Sampson, C.R., Seybold, M.G., 2011. An automated, objective, multi-satellite platform tropical cyclone surface wind analysis. J. Appl. Meteorol. Climatol. 50, 2149–2166. https://doi.org/10.1175/2011JAMC2673.1.

Knaff, J.A., Longmore, S.P., Molenar, D.A., 2014. An objective satellite-based tropical cyclone size climatology. J. Clim. 27, 455–476. https://doi.org/10.1175/JCLI-D-13-00096.1.

Knaff, J.A., Sampson, C.R., Musgrave, K.D., 2018. Statistical tropical cyclone wind radii prediction using climatology and persistence: updates for the western North Pacific. Wea. Forecast. 33, 1093–1098. https://doi.org/10.1175/WAF-D-18-0027.1.

Knaff, J.A., Sampson, C.R., Kucas, M.E., Slocum, C.J., Brennan, M.J., Meissner, T., Ricciardulli, L., Mouche, A., Reul, N., Morris, M., Chirokova, G., Caroff, P., 2021. Estimating tropical cyclone surface winds: current status, emerging technologies, historical evolution, and a look to the future. Trop. Cyclone Res. Rev. 10, 125–150. https://doi.org/10.1016/j.tcrr.2021.09.002.

Knutson, T.R., Sirutis, J.J., Zhao, M., Tuleya, R.E., Bender, M., Vecchi, G.A., Villarini, G., Chavas, D., 2015. Global projections of intense tropical cyclone activity for the late twenty-first century from dynamical downscaling of CMIP5/RCP4.5 scenarios. J. Clim. 28, 7203–7224. https://doi.org/10.1175/JCLI-D-15-0129.1.

Kreussler, P., Caron, L.-P., Wild, S., Loosveldt Tomas, S., Chauvin, F., Moine, M.-P., Coauthors, 2021. Tropical cyclone integrated kinetic energy in an ensemble of HighResMIP simulations. Geophys. Res. Lett. 48, e2020GL090963. https://doi.org/10.1029/2020GL090963.

Landsea, C.W., Franklin, J.L., 2013. Atlantic hurricane database uncertainty and presentation of a new database format. Mon. Wea. Rev. 141, 3576–3592. https://doi.org/10.1175/MWR-D-12-00254.1.

Li, Y., Tang, Y., Wang, S., 2022. Rapid growth of outer size of tropical cyclones: a new perspective on their destructive potential. Geophys. Res. Lett. 49, e2022GL099230. https://doi.org/10.1029/2022GL099230.

Lin, N., Lane, P., Emanuel, K.A., Sullivan, R.M., Donnelly, J.P., 2014. Heightened hurricane surge risk in northwest Florida revealed from climatological-hydrodynamic modeling and paleorecord reconstruction. J. Geophys. Res. Atmos. 119, 8606–8623. https://doi.org/10.1002/2014JD021584.

Liu, K., Chan, J.C.L., 1999. Size of tropical cyclones as inferred from ERS-1 and ERS-2 data. Mon. Wea. Rev. 127, 2992–3001. https://10.1175/1520-0493(1999)127,2992.SOTCAI.2.0.CO;2.

Lu, K., Chavas, D., 2022. Tropical cyclone size is strongly limited by the Rhines scale: experiments with a barotropic model. J. Atmos. Sci. 79, 2109–2124. https://doi.org/10.1175/JAS-D-21-0224.1.

Ma, C., Peng, M., Li, T., Coauthors, 2019. Effects of background state on tropical cyclone size over the western North Pacific and northern Atlantic. Clim. Dyn. 52, 4143–4156. https://doi.org/10.1007/s00382-018-4372-3.

Martinez, J., Nam, C.C., Bell, M.M., 2020. On the contributions of incipient vortex circulation and environmental moisture to tropical cyclone expansion. J. Geophys. Res. Atmos. 125, e2020JD033324. https://doi.org/10.1029/2020JD033324.

Matyas, C.J., 2010. Associations between the size of hurricane rain fields at landfall and their surrounding environments. Meteorol. Atmos. Phys. 106, 135–148. https://doi.org/10.1007/s00703-009-0056-1.

Matyas, C.J., Zick, S.E., Tang, J., 2018. Using an object-based approach to quantify the spatial structure of reflectivity regions in Hurricane Isabel (2003). Part I: comparisons between radar observations and model simulations. Mon. Wea. Rev. 146, 1319–1340. https://doi.org/10.1175/mwr-d-17-0077.

McCaul, E., 1991. Buoyancy and shear characteristics of hurricane-tornado environments. Mon. Wea. Rev. 119, 1954–1978. https://doi.org/10.1175/1520-0493(1991)119,1954.BASCOH.2.0.CO;2.

Merrill, R.T., 1984. A comparison of large and small tropical cyclones. Mon. Wea. Rev. 112, 1408–1418. https://doi.org/10.1175/1520-0493(1984)112,1408.ACOLAS.2.0.CO;2.

Mok, D.K.H., Chan, J.C.L., Chan, K.T.F., 2018. A 31-year climatology of tropical cyclone size from the NCEP Climate Forecast System Reanalysis. Int. J. Climatol. 38, e796–e806. https://doi.org/10.1002/joc.5407.

NHC, 2017. Arrival of Tropical-Storm-Force Winds Graphics [available online at: https://www.nhc.noaa.gov/experimental/arrivaltimes/toapdd.pdf.

Paredes, M., Schenkel, B.A., Edwards, R., Coniglio, M., 2021. Tropical cyclone outer size impacts the number and location of tornadoes. Geophys. Res. Lett. 48. https://doi.org/10.1029/2021GL095922 e2021GL095922.

Parker, C.L., Bruyère, C.L., Mooney, P.A., Coauthors, 2018. The response of land-falling tropical cyclone characteristics to projected climate change in northeast Australia. Clim. Dyn. 51, 3467–3485. https://doi.org/10.1007/s00382-018-4091-9.

Patricola, C.M., Wehner, M.F., 2018. Anthropogenic influences on major tropical cyclone events. Nature 563, 339–346. https://doi.org/10.1038/s41586-018-0673-2.

Rappin, E.D., Nolan, D.S., 2012. The effect of vertical shear orientation on tropical cyclogenesis. Quart. J. Roy. Meteorol. Soc. 138, 1035–1054. https://doi.org/10.1002/qj.977.

Reed, K.A., Chavas, D.R., 2015. Uniformly rotating global radiative-convective equilibrium in the Community Atmosphere Model, version 5. J. Adv. Model. Earth Syst. 7, 1938–1955. https://doi.org/10.1002/2015MS000519.

Rhines, P.B., 1975. Waves and turbulence on a beta-plane. J. Fluid Mech. 69, 417–443. https://doi.org/10.1017/S0022112075001504.

Sampson, C.R., Schrader, A.J., 2000. The automated tropical cyclone forecasting system (version 3.2). Bull. Amer. Meteorol. Soc. 81, 1231–1240. https://doi.org/10.1175/1520-0477(2000)081%3C1231.TATCFS%3E2.3.CO;2.

Sampson, C.R., Fukada, E.M., Knaff, J.A., Strahl, B.R., Brennan, M.J., Marchok, T., 2017. Tropical cyclone gale wind radii estimates for the western North Pacific. Wea. Forecasting 32, 1007–1028. https://doi.org/10.1175/WAF-D-16-0196.1.

Sampson, C.R., Goerss, J.S., Knaff, J.A., Strahl, B.R., Fukada, E.M., Serra, E.A., 2018. Tropical cyclone gale wind radii estimates, forecasts, and error forecasts for the western North Pacific. Wea. Forecast. 33, 1081–1092. https://doi.org/10.1175/WAF-D-17-0153.1.

Santos, P., DeMaria, M., Ostwald, O., DeMaria, G., Onderlinde, M., 2021. A Gridded Version of the National Hurricane Center Official Forecasts to Support Operations at National Centers and Weather Forecast Offices (WFOs): Calibration and Bias Correction. 101st AMS Annual Meeting, Virtual, 14.1. Amer. Meteor. Soc.

Schenkel, B.A., Lin, N., Chavas, D., Oppenheimer, M., Brammer, A., 2017. Evaluating outer tropical cyclone size in reanalysis datasets using QuikSCAT data. J. Clim. 30, 8745–8762. https://doi.org/10.1175/JCLI-D-17-0122.1.

Schenkel, B.A., Lin, N., Chavas, D., Vecchi, G., Oppenheimer, M., Brammer, A., 2018. Lifetime evolution of outer tropical cyclone size and structure as diagnosed from reanalysis and climate model data. J. Clim. 31, 7985–8004. https://doi.org/10.1175/JCLI-D-17-0630.1.

Schenkel, B.A., Chavas, D., Lin, N., Knutson, T., Vecchi, G., Brammer, A., 2023. North Atlantic Tropical Cyclone Outer Size and Structure Remain Unchanged by the Late Twenty-First Century. J. Clim. 36, 359–382. https://doi.org/10.1175/JCLI-D-22-0066.1.

Stansfield, A.M., Reed, K.A., 2021. Tropical cyclone precipitation response to surface warming in aquaplanet simulations with uniform thermal forcing. J. Geophys. Res. Atmos. 126, e2021JD035197. https://doi.org/10.1029/2021JD035197.

Stansfield, A.M., Reed, K., Zarzycki, C.M., 2020. Changes in precipitation from North Atlantic tropical cyclones under RCP scenarios in the variable-resolution community atmosphere model. Geophys. Res. Lett. 47, e2019GL086930. https://doi.org/10.1029/2019GL086930.

Stiles, B., Coauthors, 2014. Optimized tropical cyclone winds from QuikSCAT: a neural network approach. IEEE Trans. Geosci. Remote Sens. 52, 7418–7434. https://doi.org/10.1109/TGRS.2014.2312333.

Wang, S., Toumi, R., 2018a. A historical analysis of the mature stage of tropical cyclones. Int. J. Climatol. 38, 2490–2505. https://doi.org/10.1002/joc.5374.

Wang, S., Toumi, R., 2018b. Reduced sensitivity of tropical cyclone intensity and size to sea surface temperature in a radiative-convective equilibrium environment. Adv. Atmos. Sci. 35, 981–993. https://doi.org/10.1007/s00376-018-7277-5.

Wang, D., Lin, Y., Chavas, D.R., 2022. Tropical cyclone potential size. J. Atmos. Sci. 79, 3001–3025. https://doi.org/10.1175/JAS-D-21-0325.1.

Wang, S., Toumi, R., 2019. Impact of dry midlevel air on the tropical cyclone outer circulation. J. Atmos. Sci. 76, 1809–1826. https://doi.org/10.1175/JAS-D-18-0302.1.

Wang, S., Toumi, R., 2022 Jun 9. An analytic model of the tropical cyclone outer size. npj Atmos. Clim. Sci. 5 (1), 46.

Wang, S., Toumi, R., 2021. Recent tropical cyclone changes inferred from ocean surface temperature cold wakes. Sci. Rep. 11, 22269. https://doi.org/10.1038/s41598-021-01612-9.

Weatherford, C.L., Gray, W.M., 1988. Typhoon structure as revealed by aircraft reconnaissance. Part I: data analysis and climatology. Mon. Wea. Rev. 116, 1032–1043. https://doi.org/10.1175/1520-0493(1988)116,1032.TSARBA.2.0.CO;2.

Xu, J., Wang, Y., 2010. Sensitivity of the simulated tropical cyclone inner-core size to the initial vortex size. Mon. Wea. Rev. 138, 4135–4157. https://doi.org/10.1175/WAF-D-14-00141.1.

Yamada, Y., Satoh, M., Sugi, M., Kodama, C., Noda, A.T., Nakano, M., Nasuno, T., 2017. Response of tropical cyclone activity and structure to global warming in a high-resolution global nonhydrostatic model. J. Clim. 30, 9703–9724. https://doi.org/10.1175/JCLI-D-17-0068.1.

Yang, N., Li, Y., Chan, J.C.L., Cheung, K.K.W., Ye, L., Wu, Y., 2022. Vertical variation of tropical cyclone size in the western North Pacific. Int. J. Climatol. 42, 4424–4444. https://doi.org/10.1002/joc.7477.

Zhang, K., Chan, K.T.F., 2023. An ERA5 global climatology of tropical cyclone size asymmetry. Int. J. Climatol. 43, 950–963. https://doi.org/10.1002/joc.7846.

Zhang, J., Lin, Y., Chavas, D.R., Mei, W., 2019. Tropical cyclone cold wake size and its applications to power dissipation and ocean heat uptake estimates. Geophys. Res. Lett. 46, 10177–10185. https://doi.org/10.1029/2019GL083783.

Zhang, J.A., Dunion, J.P., Nolan, D.S., 2020. In situ observations of the diurnal variation in the boundary layer of mature hurricanes. Geophys. Res. Lett. 47, 2019GL086206. https://doi.org/10.1029/2019GL086206.

Zhang, B., Zhu, Z., Perrie, W., Tang, J., Zhang, J.A., 2021. Estimating tropical cyclone wind structure and intensity from spaceborne radiometer and synthetic aperture radar. IEEE J. Selected Top. Appl. Earth Observations Remote Sensing 14, 4043–4050. https://10.1109/JSTARS.2021.3065866.

Zhou, Y., Matyas, C., Li, H., Tang, J., 2018. Conditions associated with rain field size for tropical cyclones landfalling over the Eastern United States. Atmos. Res. 214, 375–385. https://doi.org/10.1016/j.atmosres.2018.08.019.

Zhuo, J., Tan, Z., 2021. Physics-augmented deep learning to improve tropical cyclone intensity and size estimation from satellite imagery. Mon. Wea. Rev. 149, 2097–2113. https://doi.org/10.1175/MWR-D-20-0333.1.

Zick, S., Matyas, C., Lackmann, G., Tang, J., Bennett, B., 2022. Illustration of an object-based approach to identify structural differences in tropical cyclone wind fields. Quart. J. Roy. Meteorol. Soc. 48, 2587–2606. https://doi.org/10.1002/qj.4326.